Title

Bioengineered scaffolds for 3D culture demonstrate extracellular matrix-mediated mechanisms of chemotherapy resistance in glioblastoma

Authors

Xiao, Weikun
Wang, Shanshan
Zhang, Rongyu
et al.

Publication Date

2020

DOI

10.1016/j.matbio.2019.04.003

Peer reviewed

Bioengineered scaffolds for 3D culture demonstrate extracellular matrix-mediated mechanisms of chemotherapy resistance in glioblastoma

Weikun Xiao, Shanshan Wang, Rongyu Zhang, Alireza Sohrabi, Qi Yu, Sihan Liu, Arshia Ehsanipour, Jesse Liang, Rebecca D. Bierman, David A. Nathanson, Stephanie K. Seidlits

PII: S0945-053X(19)30022-8
DOI: https://doi.org/10.1016/j.matbio.2019.04.003
Reference: MATBIO 1562

To appear in: *Matrix Biology*

Received date: 12 January 2019
Revised date: 17 April 2019
Accepted date: 19 April 2019

Please cite this article as: W. Xiao, S. Wang, R. Zhang, et al., Bioengineered scaffolds for 3D culture demonstrate extracellular matrix-mediated mechanisms of chemotherapy resistance in glioblastoma, Matrix Biology, https://doi.org/10.1016/j.matbio.2019.04.003

Title: Bioengineered scaffolds for 3D culture demonstrate extracellular matrix-mediated mechanisms of chemotherapy resistance in glioblastoma

Authors: Weikun Xiao[1], Shanshan Wang[1], Rongyu Zhang[1], Alireza Sohrabi[1], Qi Yu[1], Sihan Liu, [1] Arshia Ehsanipour[1], Jesse Liang[1], Rebecca D. Bierman[1], David A. Nathanson[2,3], Stephanie K. Seidlits[1,2,4,5]

Affiliations:

[1]Department of Bioengineering, [2]Jonsson Comprehensive Cancer Center, [3]Department of Molecular and Medical Pharmacology, [4]Broad Stem Cell Research Center, [5]Brain Research Institute

University of California Los Angeles, Los Angeles CA USA 90095

Corresponding Author:

Stephanie Seidlits, Ph.D.
Asst. Prof. of Bioengineering
420 Westwood Plaza, 5121H
University of California, Los Angeles
Los Angeles, CA, 90095
310-267-5244
seidlits@g.ucla.edu

Keywords: Hyaluronic acid, Drug resistance, Extracellular matrix, 3D culture, Integrin, CD44, Src, Glioblastoma, Cilengitide, Dasatinib, Chemotherapy, BCL-2 family

Abstract:

Originating in the brain, glioblastoma (GBM) is a highly lethal and virtually incurable cancer, in large part because it readily develops resistance to treatments. While numerous studies have investigated mechanisms enabling GBM cells to evade chemotherapy-induced apoptosis, few have addressed how their surrounding extracellular matrix (ECM) acts to promote their survival. Here, we employed a biomaterial-based, 3D culture platform to investigate systematically how interactions between patient-derived GBM cells and the brain ECM promote resistance to alkylating chemotherapies — including temozolomide, which is used routinely in clinical practice. Scaffolds for 3D culture were fabricated from hyaluronic acid (HA) — a major structural and bioactive component of the brain ECM — and functionalized with the RGD (arginine-glycine-aspartic acid) tripeptide to provide sites for integrin engagement. Data demonstrate that cooperative engagement of CD44, through HA, and integrin α_V, through RGD, facilitates resistance to alkylating chemotherapies through co-activation of Src, which inhibited downstream expression of BCL-2 family pro-apoptotic factors. In sum, a bioengineered, 3D culture platform was used to gain new mechanistic insights into how ECM in the brain tumor microenvironment promotes resistance to chemotherapy and suggests potential avenues for the development of novel, matrix-targeted combination therapies designed to suppress chemotherapy resistance in GBM.

Graphical Abstract:

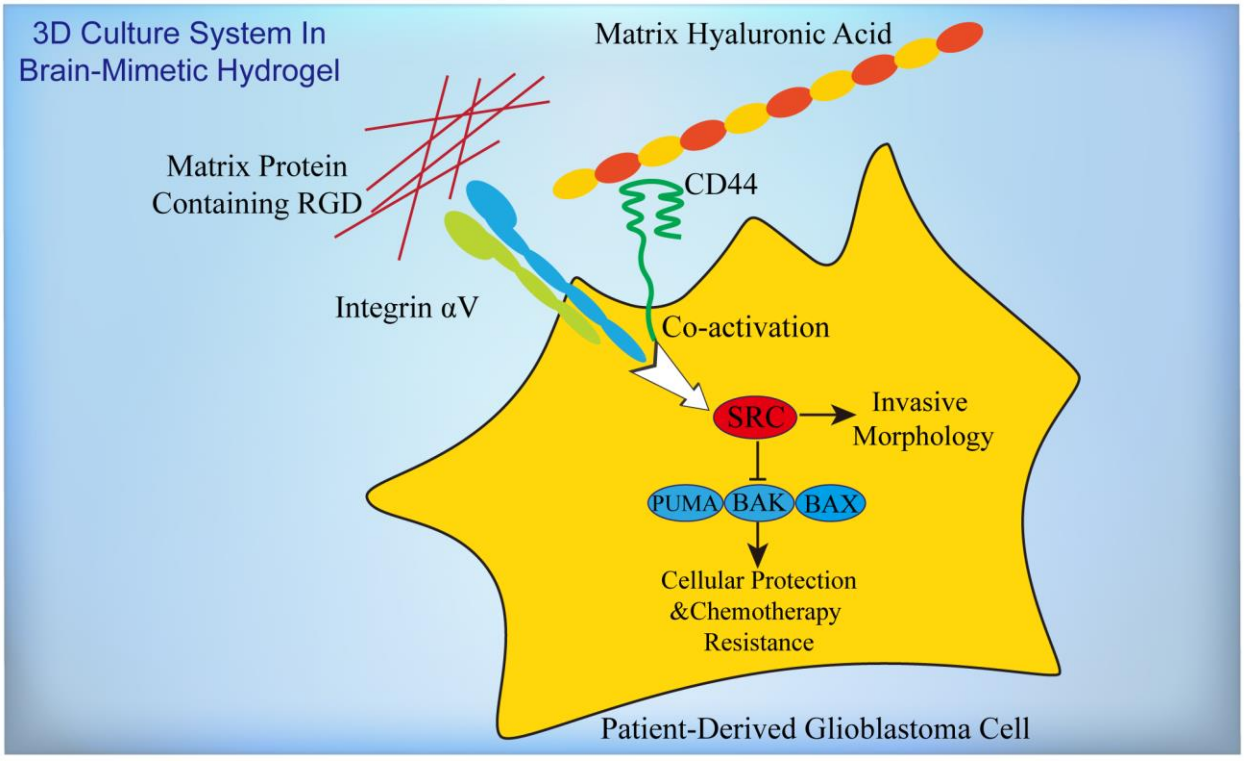

Highlights:

Hyaluronic acid (HA) and RGD-containing proteins in the extracellular matrix (ECM) interact with integrin and CD44 receptors, respectively, on patient-derived glioblastoma (GBM) cells to promote upregulation of Src in novel 3D hydrogel cultures.

Matrix-mediated Src activation promotes invasive morphologies and deregulates expression of pro-apoptotic factors induced by chemotherapies in GBM.

HA and adhesive proteins in the ECM protect GBM cells from chemotherapy-induced apoptosis.

Combinatorial treatment with chemotherapy dasatinib, which inhibits Src phosphorylation, provides a promising strategy to overcome matrix mediated drug resistance in GBM.

1. Introduction:

Glioblastoma (GBM) is the most common, yet lethal, cancer originating in the central nervous system[1,2]. Its lethality stems from its robust resistance to treatment and aggressive infiltration of healthy tissue[1]. The alkylating chemotherapy temozolomide (TMZ) is routinely used as an adjuvant chemotherapy following surgical resection of tumors and post-surgery radiotherapy. Although less common than TMZ treatment, biodegradable wafers, which continuously deliver the alkylating chemotherapy agent carmustine (also known as BCNU), have also been used widely for GBM treatment. Unfortunately, even with treatment the median survival of GBM patients is only 12-15 months[3].

The important role of the extracellular matrix (ECM) in treatment resistance has been indicated in several cancers. For example, CD44 activation through hyaluronic acid (HA) has been reported to support cancer growth, resistance and metastasis[4–6]. Likewise, cell-adhesive proteins in the ECM, in particular those containing the integrin-binding RGD (arginine-glycine-aspartic acid) motif, mediate downstream signaling pathways associated with cancer cell survival and invasion[7]. In GBM, elevated expression of the ECM components — including the glycosaminoglycan hyaluronic acid (HA) and several cell-adhesive proteins — and their corresponding cell surface receptors — CD44 and integrins, respectively — has been frequently reported to correspond with disease progression[7–10]. ECM engagement with either integrin or CD44 receptors has been reported to activate Src protein-tyrosine kinase (Src) in [11–13]. In sarcoma and ovarian cancer, Src has been observed as a modulator of treatment sensitivity, where its inhibition by dasatinib promoted chemotherapy-induced apoptosis[14,15]. In GBM, a number of studies have found correlations between Src hyper-activation and tumorigenesis, invasion and progression [11,12,15,16]. However, these previous studies were largely focused on elucidating the role of Src in GBM invasion and how Src activation may influence treatment response in GBM remains largely unknown.

Despite a growing body of evidence indicating that ECM in the GBM tumor microenvironment facilitates therapeutic resistance, it has been a technical challenge to investigate the underlying mechanisms of this influence in a systematic and detailed manner. While *in vivo* studies can provide valuable information, the ubiquitous nature of most ECM components, and their respective receptors, throughout organ systems makes it difficult to isolate independent effects of specific ECM-tumor cell interactions on tumor behavior and necessitates the use of a simplified, *ex vivo* system. However, common approaches for experimental culture do not provide GBM cells with adequate microenvironmental support to preserve their physiology [17].

For example, previous studies of cell-ECM interactions have relied heavily on non-specific adsorption of large ECM biomolecules, resulting in uncontrolled protein denaturation, onto two-dimensional (2D) culture substrates with stiffness orders of magnitude harder than normal brain or tumor tissues[18]. Gliomasphere (GS) cultures, where GBM tumor spheroids are cultured in suspension have also been widely used[19]. While GS cultures provide a more realistic, 3D microenvironment for intercellular interactions than 2D monolayers, they do not provide any control over the surrounding ECM microenvironment, which includes biochemical and biomechanical features.

Here, we employed hydrogel biomaterials that surround 3D cultured, patient-derived GBM cells with a bioengineered matrix composed of HA and integrin-binding sites based on the "RGD" adhesive tripeptide. As the mechanical microenvironment can also have profound effects on tumor cells[8,20], hydrogel matrices were designed to approximate the mechanical properties of native brain. Previously, we demonstrated that patient-derived GBM cells cultured in these tunable, 3D culture matrices better approximated responses to therapeutic inhibition of epidermal growth factor receptor (EGFR) observed in patient-matched, orthotopic xenografts than did patient-matched GS cultures [21]. Here, we used these hydrogel cultures to demonstrate that CD44-HA and integrin-RGD interactions act together to drive chemotherapy resistance. Furthermore, we have identified Src activation as a key signaling event mediating both chemotherapy resistance and invasive morphology. Finally, we demonstrate that ECM components act to protect GBM cells from chemotherapy-induced apoptosis through downstream, Src-mediated inhibition of BCL-2 family pro-apoptotic factors.

2. Methods:

All reagents were purchased from ThermoFisher unless otherwise stated.

Fabrication of hydrogel matrices: Hyaluronic acid (HA, average molecular weight 700kDa, LifeCore Biomedical, Chaska, MN, USA) was thiolated (~5% of the repeating disaccharide units), as previously described[21,22]. Maleimide-terminated 4-arm polyethylene glycol (4-arm-PEG-Mal, 20kDa) from Laysan Bio (Arab, AL, USA) was resuspended at 12.5mg/ml in phosphate buffered saline (PBS, MilliporeSigma, Temecula, CA, USA). L-Cysteine (MilliporeSigma) or RGD peptide (customized sequence N-Ac-GCGYGRGDSP-COOH from Genscript, Piscataway, NJ, USA) was reconstituted in PBS (2.81 mM), then mixed with 4-arm-PEG-Mal solution at a 2:1 molar ratio to achieve 150 μM of final concentration of peptide or L-cysteine. Thiolated HA was dissolved at 13.3 mg/mL in 20 mM HEPES buffer and adjusted to around pH 7 before mixing with 5 mg/mL thiol-terminated 4-arm-poly ethylene glycol (4-arm-PEG-SH, 20kDa, Laysan Bio, Arab, AL, USA) at a 3:1 volume ratio. Finally, an equal volume of 4-arm-PEG-Mal solution was mixed with thiolated HA/4-arm-PEG-SH solution (total of 80 μl) in a silicone mold (Grace Biolabs, Bend, OR, USA).

Patient-derived GBM cell lines: GBM cell lines derived from patients (HK301, GBM6, GS024, and GS025) were used. HK301 was generously provided Dr. Harley Kornblum at UCLA and was collected in April 2010. GS024 and GS025 were collected in March 2015. GBM6 was collected in span of 1999-2006[23]. GS024, GS025 and HK301 were collected with approval and according to guidelines from the UCLA Institutional Review Board protocol 10-000655 [24]. HK301 cells were used between passages 15 and 25, GBM6 were used between passages 10 and 15, and GS024 and GS025 were used between passages 4 and 9. All cell lines were verified through short tandem repeat analysis[25].

Gliomasphere culture: GBM cells (50,000/mL) were cultured in suspension in DMEM/F12 with 1x G21 (Gemini Bio-Products, West Sacramento, CA, USA), 1% penicillin/streptomycin, 50 ng/mL epidermal growth factor (EGF) (PeproTech, Rocky Hill, NJ, USA), 20 ng/ml fibroblast growth factor-basic (FGF-2) (PeproTech), and 25 μg/mL heparin (MilliporeSigma, St. Louis, MO, USA). Cultures were routinely tested for mycoplasma contamination (C7028, Thermo Fisher Scientific, Waltham, MA, USA). TrypLE Express (1 mL) was used to dissociate GS once they reached approximately 200 μm in diameter. Dissociated cells were passed through a 70 μm cell strainer to remove any remaining aggregates before re-seeding into suspension culture. To establish hydrogel cultures, dissociated, single cells were resuspended (1 million cells/mL) in approximately 12 mg/mL of peptide-modified PEG-maleimide solution prior to mixing the HA-thiol/PEG-thiol solution to initiate crosslinking, which occurs rapidly at 37ºC. Cell culture medium was added to cover the hydrogel cultures 10 min. after mixing.

Viral transduction: shCD44-2 pRRL was a gift from Bob Weinberg (Addgene Plasmid #19123). GIPZ Human ITGAV shRNA (Clone Id: V2LHS_133468) lentiviral vector glycerol stock was purchased from Dharmacon, Inc. (Lafayete, CO). Lentivirus was produced using the human embryonic kidney (HEK Lenti 293T) cell line (Takara Bio USA, Mountain View, CA). A third-generation packaging system was used to produce the lentivirus[26]. Virus was added to cell culture in 6-well plate with multiplicity of infection of 2000. Fresh medium was replaced 24 hrs after infection. Cells were allowed to grow for another 48 hrs before encapsulation.

Drug treatment: Temozolomide (TMZ), carmustine, cilengitide, and dasatinib were purchased from MilliporeSigma. TMZ and dasatinib were prepared in DMSO at 100 mM and 10 mM, respectively. Carmustine was dissolved in ethanol at 100 mM, and cilengitide was in PBS at 10mM. Final working concentrations of each compound were: 500 μM TMZ, 100 μM carmustine for the GBM6 cell line, 50 μM carmustine for all other cell lines, 100 nM dasatinib and 50 μM cilengitide. Working concentrations of TMZ and carmustine were determined by IC50 for each cell line. All vehicle groups in the treatment had equivalent amounts of DMSO, ethanol, or PBS added to culture media.

Bioluminescence imaging of live cultures: GBM cells were transduced with lentivirus encoding for constitutive expression of firefly luciferase, as previously described[21]. D-luciferin (1 mM) was added to the culture medium 1 hr prior to imaging. Bioluminescence signal was imaged using an IVIS Illumina II (PerkinElmer, Waltham, MA, USA) with a 4-5 mins exposure. All readings are normalized to background intensity and area. Relative luminescence units (RLU), photon intensity corrected for background and noise of the detector, for experimental groups at each time point were normalized to RLU from samples in vehicle groups and RLU at day 0.

Hydrogel culture cryopreservation, immunostaining, and imaging: Hydrogel cultures were fixed in 4% para-formaldehyde (PFA) at 4^{o}C overnight. The next day, the hydrogels were incubated serially in solutions with increasing concentrations of sucrose in PBS (5-20 wt%). On third day, the hydrogels were embedded in 20 wt% sucrose in O.C.T. and flash frozen in 2-methylbutane. Frozen samples were stored at -80^{o}C until cryosectioning into 18 μm sections, as previously described[22]. The sections were fixed in 4% PFA for 10 min. and washed in tris-buffered saline (TBS) before blocking using 1% bovine serum albumin (BSA) and 5% normal donkey serum for 1hr at room temperature. Primary antibodies, diluted in blocking buffer, were incubated with sections at 4^{o}C overnight. The next day, the slides were washed in TBS. Appropriate secondary antibodies and Hoescht 33342 were diluted in TBS and incubated with sections at room temperature for 45 min. Finally, sections were washed in TBS and mounted with coverslips

using fluoromount G (Southern Biotech, Birmingham, AL, USA). All samples were imaged with Zeiss Axio-Observer microscope (Carl Zeiss, Oberkochen, Germany). All fluorescent images within the same comparison groups were imaged with same parameters, and all samples within each comparison group were prepared and processed together. For details on antibodies used, please see **Supplementary Table 1**.

Western blotting: Hydrogel cultures were placed in 1.5 mL microcentrifuge tubes. 100 µL RIPA buffer with 1x protease/phosphatase inhibitors (MilliporeSigma) were incubated with the hydrogels on ice. A 1 mL syringe attached with 20G needle was used to homogenize the sample. The mixture was then incubated on ice for an additional 15 min. For GS cultures, dissociated cells were centrifuged at 500xg for 5 min. followed by resuspension with complete RIPA buffer with 1x protease/phosphatase inhibitors on ice, and the mixture was incubated on ice for 15 min. with occasional vortexing. All samples were centrifuged 14,000xg for 15 min. Supernatants were collected and 1:1 mixed with laemmli buffer with 5% 2-mercaptoethanol. SDS-PAGE was performed using a 12-well, 4-12% bis-tris gradient gel in a mini blot module under 1x MOPS buffer. Protein was transferred from the SDS-PAGE gel to a PVDF membrane in 1x transfer buffer under 20V for 100 min. Blots were blocked in 5% BSA in TBS with 0.1% tween (TBST) for 1hr at room temperature, and then incubated with primary antibodies diluted in blocking buffer at 4^{o}C overnight. The next day, blots were washed with TBST, before incubating with secondary antibody diluted in 5% BSA in TBST for 1hr at room temperature. After additional washes in TBST, blots were incubated in Clarity Western ECL Substrates (Bio-Rad, Hercules, CA, USA) for 3 min. and imaged in MyECL Imager. For the list of antibodies, information on working dilutions and expected molecular weights used in the study, please see **Supplementary Table 1** For original chemiluminescence blot images marked with molecular weight ladders, please see **Figure S1**.

Flow cytometry for analysis of proliferation: To measure percentage of cell population that has actively undergone proliferation, 5-ethynyl-2'deoxyuridine (EdU, 10µM, Abcam, Cambridge UK) was added to culture medium and incubated in 37^{o}C for 2.5 hrs. Hydrogel or gliomasphere cultures were then placed in 1mL of TrypLE Express at 37 ^{o}C for 5 min. before adding 4 mL of 1% BSA in PBS to the reaction mixture. For hydrogel cultures, the mixture was passed through a 20 G needles at least 8 times gently. Cell suspensions from both hydrogel and gliomapshere cultures then were filtered through a 70 µm cell strainer. An additional 5mL of 1% BSA in PBS was used to wash the cell strainer and collect any remaining cells. The mixture was centrifuged at 500 x g for 5 min., and the supernatant removed. The cell pellet was resuspended in 100 µL of 4% PFA and incubated for 15 min, before washing with 3 mL of 1%BSA in PBS. Fixed cells were permeabilized in 100 µL of 0.1% saponin (MilliporeSigma) in 1% BSA in PBS for 15 min., followed by an additional 500 µL of 100 mM sodium ascorbate, 2mM $CuSO_4$ and 1µM Alexa Fluor 647 Azide in PBS for 30 min. in the dark. Finally, cells were washed with 3 mL of 0.1% saponin and 1% BSA in PBS and resuspended in 500 µL of washing buffer. Data were collected using Fortessa LSRII flow cytometer (BD Biosciences, Franklin Lakes, NJ, USA) and were analyzed using FlowJo software. EdU positive cell population represents percentage of cells have gone through S phase of cell division during the 2.5 hr period of exposure to EdU in culture.

Statistical Analysis: Statistical analysis was performed by using GraphPad Prism software (La Jolla, CA, USA). In most cases, student's *t* test or ANOVA with Tukey's post-hoc comparisons

were used to determine statistical significance. More details and any deviations from this procedure are provided in figure captions when applicable.

3. Results:

3.1 High HA scaffolds facilitate chemotherapy resistance

We employed a 12-day treatment protocol where cells were exposed to two treatment cycles — 3 days with drug followed by 3 days without — to approximate treatment cycles used for TMZ chemotherapy in clinical practice[27] (**Fig. 1A**). Drug response was observed in patient-derived GBM cells cultured in 3D hydrogels fabricated with either high (0.5% w/v) or low (0.1% w/v) HA content, as previously described[21]. After 12 days in culture HK301 cells formed spheroid aggregates with similar morphologies in both scaffold conditions without treatment (vehicle control) and high HA scaffolds wither treatment (TMZ or carmustine) (**Fig. 1B**). In contrast, cell aggregates were clearly smaller in low HA scaffolds with treatment. Growth kinetics of scaffold cultures tracked over time through bioluminescence imaging of a constitutively overexpressing luciferase reporter confirmed that HK301 cells in high HA hydrogels had grown significantly more than those in other conditions, starting at day 6 of the treatment scheme (**Fig. 1C**). No obvious differences in cell morphology or aggregation were observed with scaffold type or treatment for GBM6 cells (*data not shown*). The exact number of days before resistance was observed in GBM6 cultures were highly variable across independent experimental trails (**Fig. S2A**). However, quantification of the bioluminescence signal from treated cultures, normalized to that from untreated, at the end of the treatment on day 12 confirmed that both HK301 and GBM6 cells cultured in high HA hydrogels were less responsive to alkylating chemotherapies than those cultured in low HA content hydrogels or as GS (**Fig. 1D**).

In clinical cases, a cycle of TMZ chemotherapy is typically defined as 5 days of treatment followed 23 days of not treatment, or “rest”[3]. During this “rest” period, tumors have the opportunity to recover, adapt and/or grow. Here, we applied 3 days of treatment followed by 3 days of “rest”. During the first “rest” period (days 3-6), tumor cell cultures appeared to switch to a state that was less responsive to treatment with either TMZ or carmustine and average growth rates were more similar to untreated controls (**Fig. 1C**).

3.2 Matrix HA interacts with CD44 to protect against chemotherapy-induced apoptosis

To investigate the mechanism by which the HA-rich hydrogel scaffolds create a microenvironment that facilitates drug resistance, we first tested whether culture in hydrogels prevented DNA damage from exposure to chemotherapy agents. Using an EdU-based assay, we found that carmustine treatment reduced DNA incorporation (i.e., proliferation rate) in both high HA hydrogel and GS cultures as measured on the 3rd day of carmustine treatment (**Fig. 2A; Fig. S2B**). TMZ treatment had a similar cytostatic effect on cultures in high HA (**Fig. S2C**). When GS were treated with either drug, too few cells remained to perform reliable measurements of EdU incorporation via flow cytometry (*data not shown*). Although carmustine treatment attenuated cell proliferation in both hydrogel scaffold and GS cultures, proliferation in GS was essentially halted while some proliferation persisted in hydrogel cultures, prompting further investigation.

Alkylating agents induce cell cycle arrest, eventually leading to programmed cell death, or apoptosis[28]. Thus, we suspected hydrogel-cultured cells may have gained resistance to the cytostatic effects of carmustine via reduced cytotoxicity. As predicted, when treated with

carmustine, relative expression of cleaved poly ADP ribose polymerase (cl-PARP), a marker for late-stage apoptosis, in HK301 cells was higher in GS than in high HA hydrogel cultures (**Fig. 2B**). This comparison could not be made with GBM6 cells, as too many cells died with treatment to make it possible to collect lysate for Western blotting. By comparing cl-PARP expression in high and low HA hydrogel cultures of HK301 cells, we further confirmed that increased HA content led to a reduction in apoptosis (i.e., cl-PARP expression) in response to treatment (**Fig. 2C, Fig. S3A**). To evaluate the contribution of the CD44 receptor to anti-apoptotic protection provided by the HA matrix, we repeated experiments with GBM cells transduced with shRNA to knockdown CD44 expression. Treatment-induced apoptosis increased significantly with the CD44 knockdown (**Fig. 2D, Fig. S3B**). No treatment (vehicle) controls confirmed that the CD44 knockdown alone was not sufficient to induce cl-PARP expression.

3.3 The RGD motif and HA synergistically protect against treatment-induced apoptosis

The integrin-binding RGD motif is found in many ECM proteins, and cell adhesion through RGD has been reported to promote survival and invasion in GBM[29]. Our hydrogel system enables incorporation of ECM-mimetic peptides containing RGD to recapitulate cell-ECM interactions through which biochemical and biomechanical cues may be transduced [21,22]. After GBM cell encapsulation into RGD-incorporated hydrogels, the majority of cells displayed an invasive morphology resembling a multicellular, or collective, migration mode (**Fig. 3A; Fig. S4**). In contrast, cells remained as spheroid aggregates when cultured in hydrogels lacking the RGD motif. When treated with TMZ or carmustine, incorporation of RGD provided additional protection against apoptosis, significantly reducing cl-PARP expression over that in high HA scaffolds without RGD (**Fig. 3B, Fig. S3C**). To further evaluate the role of immobilized RGD in hydrogel matrices, we treated cells with both an alkylating chemotherapy and cilengitide, or cyclo-RGD. Cilengitide was originally developed as a targeted therapy for GBM which acts through selective disruption of integrin αV interaction with RGD-containing ECM proteins[30]. In HA-rich hydrogels with immobilized RGD peptides, addition of cilengitide competitively abolished the any invasive morphology (**Fig. 3C; Fig. S4**). While cilengitide alone did not significantly affect apoptosis, it had a synergistic action when combined with chemotherapy agents, where cl-PARP expression increased by at least 2 times (**Fig. 3D, Fig. S3D**). These results demonstrate how both HA and RGD motifs in the microenvironment can protect GBM cells from chemotherapy-induced apoptosis.

3.4 Presence of HA and RGD in hydrogel matrices induce co-expression of CD44 and integrin αV expression in 3D-cultured GBM cells

The RGD motif is reported to be a ligand for integrin αV, which undergoes hetero-dimerization with β integrin subunits upon binding[30,31]. Given that incorporation of RGD peptides into high HA hydrogels significantly enhanced chemotherapy resistance and that this effect was abolished by cilengitide treatment (**Fig. 3**), we posited that integrin αV, whose binding to RGD is selectively disrupted by cilengitide[30], and CD44 may act together to facilitate drug resistance. Immunostaining results indicated that GBM cells cultured within HA hydrogels bearing RGD co-expressed CD44 and Integrin αV within close proximity (within 0.42 μm, the effective resolution of images captured) in cell membranes — indicating possible clustering of receptors through binding to the available ECM (**Fig. 4**). Moreover, omission of HA from hydrogels or treatment of cultures with cilengitide abolished co-expression of CD44 and Integrin αV (**FIG. 4**). Together, these results indicate that direct interactions between CD44 and integrin αV may mediate chemotherapy resistance observed in HA-RGD hydrogel cultures.

3.5 Integrin αV and CD44 mediate chemotherapy resistance and invasive morphology in 3D matrices

Next, we used lentiviral vectors encoding shRNA against CD44 or integrin αV to further investigate effects of their engagement on GBM cells. Interestingly, knockdown of either CD44 or integrin αV eliminated all invasive characteristics of HK301 cells (**Fig. 5A, Fig. S3E**). However, GBM6 cells did not exhibit obvious extensions, as would be expected in invading cells (**Fig. S5**). To investigate how integrin αV affects chemotherapy-induced apoptosis, we compared cl-PARP expression between wildtype and integrin αV knockdown HK301 cells cultured in hydrogels with identical formulations. We found increased cl-PARP expression with integrin αV knockdown with carmustine treatment (**Fig. 5B, Fig. S3F**). While not statistically significant, a similar trend was observed with TMZ treatment. Through bioluminescence tracking of GBM cell growth in live cultures, the critical role of integrin αV in ECM-mediated chemotherapy resistance was confirmed (**Fig. 5C**).

3.6 HA-CD44 and RGD-integrin αV interactions act together to promote chemotherapy resistance through Src signaling

In many cancers, including GBM, Src activation is mediated by integrin binding to ECM ligands and can facilitate tumor cell invasion[15,32,33]. In addition, CD44-mediated activation of Src has been reported in colon and ovarian cancers [13,34]. Moreover, in GBM patients, Src has been identified as a downstream effector of EGFR signaling pathways, whose activation directly contributes to chemotherapy resistance[33,35]. Thus, we investigated whether CD44 and integrin αV downstream Src activation in GBM cells cultured in high HA hydrogels with RGD. With shRNA knockdown of either CD44 or integrin αV, Src phosphorylation was significantly reduced (**Fig. 6A**). Next, we confirmed that disruption of integrin-RGD binding via cilengitide treatment reduced Src activation (**Fig. 6B**). Finally, we verified that RGD and HA were both required to maximize Src phosphorylation within GBM cells in 3D culture in our engineered matrices (**Fig. 6C, D**).

Based on these results, we postulated that suppression of Src inhibition via dasatinib[16] could sensitize GBM cells to treatment, even in the presence of resistance-promoting matrix cues. First, we observed that dasatinib treatment abolished the invasive morphology of GBM cells (**Fig. 6E; Fig. S3**). Next, we found that while dasatinib alone does not induce apoptosis, dual treatment with an alkylating chemotherapy had a synergistic effect induced significantly more apoptosis (assessed by expression of cl-PARP) than treatment with either TMZ or carmustine alone (**Fig. 6F, Fig. S3G**). Consistent with these findings, dasatinib alone had no effects on culture growth (measured by bioluminescence imaging) while combination therapies resulted in a synergistic reduction in cell growth of ≥ 50% (**Fig. 6G**).

3.7 HA and RGD interactions protect GBM cells from treatment-induced apoptosis through suppression of pro-apoptotic members of the BCL-2 family

Src activation has been reported to regulate activities of BCL-2 family proteins, which direct caspase-mediated cleavage of PARP and eventually cause apoptosis[36–38]. To investigate the role of Src activation in GBM chemotherapy resistance, we examined expression of BCL-2 family pro-apoptotic factors, including P53-upregulated modulator of apoptosis (PUMA), BCL-2-associated X protein (BAX) and BCL-2 homologous antagonist killer (BAK), in all conditions. When treated with either alkylating chemotherapy, HK301 cells increased expression of PUMA, BAX, and BAK over vehicle controls (**Fig. 7A, B**). Dual treatment with either dasatinib or

cilengitide further increased this effect, while treatment with dasatinib or cilengitide alone did not alter the expression of any pro-apoptotic factors assayed (**Fig. 7A, B**). For GBM6 cells, treatment with either dasatinib or cilengitide alone elevated PUMA expression, while treatment with either alkylating chemotherapy decreased expression of all three pro-apoptotic factors (**Fig. S6A**). Notably, co-treatment with cilengitide or dasatinib rescued the expression of these pro-apoptotic factors.

Next, we evaluated the connection between upstream engagement of CD44 and integrin αV receptors by the hydrogel matrix and downstream expression of BCL-2 family pro-apoptotic factors in the presence of treatment. Chemotherapy treatment in cells with CD44 or integrin αV knockdown induced increased expression of pro-apoptotic factors (**Fig. 7C, E**; **Fig. S6B, C**). Even without treatment (i.e., vehicle), knockdown of either CD44 or integrin αV elevated expression of the pro-apoptotic factors in GBM6 cells; however, only a slight increase in expression of BAX and BAK occurred in HK301 cells (**Fig. 7C, E**). Last, we evaluated whether high HA content and RGD peptide were both required to suppress elevation of PUMA, BAX, and BAK expression with TMZ or carmustine treatment. In HK301 and GBM6 cells, the relative expressions of the pro-apoptotic factors when treated with either chemotherapy were consistent with CD44 and integrin αV knockdown results, where low HA or a lack of RGD binding sites in the matrix resulted in increased expression of pro-apoptotic factors (**Fig. 7D, E; Fig. S6 D, E**). Together, results demonstrate that cell-matrix interactions co-activated downstream Src to suppress of expression BCL-2 family pro-apoptotic factors and augment chemotherapy resistance.

4. Discussion:

The propensity of GBM to develop therapeutic resistance, where recurrence is nearly universal, is a critical area of study[1,39]. While molecular mechanisms leading to treatment insensitivity and resistance, such as MGMT methylation, have been widely investigated and despite a growing body of evidence suggesting a major role for ECM in resistance[40–42], few studies have directly evaluated the effects of ECM in the microenvironment on tumor cells. Of studies that have explored this area, the majority have relied on adsorbing purified ECM biomolecules onto hard, 2D surfaces, such as glass or tissue-culture plastic[40], or have added ECM components that do not readily adsorb, such as HA, directly to culture medium in a non-physiological, soluble form[13]. However, these methods fail to recapitulate key aspects of the tumor ECM, which is a soft, HA-rich, microporous scaffold in which cells are embedded in three dimensions. Recent studies have demonstrated that bioengineered, 3D culture systems, designed to mimic the native brain tumor ECM, can be used to study the therapeutic response of GBM cells *ex vivo* in a context that yields resistant phenotypes more similar to those observed *in vivo* than can be achieved using traditional, 2D cultures[43–48]. While the focus of the majority of previous studies has been to demonstrate feasibility and potential utility of such 3D culture platforms, here we have applied a bioengineered culture platform to elucidate detailed mechanisms of ECM-mediated treatment resistance in patient-derived GBM cells.

Here, we used a tunable, bioengineered culture platform 1) to demonstrate that the 3D microenvironment provided by the ECM facilitates acquisition of drug resistance in GBM and 2) to elucidate mechanisms underlying this phenomenon. Through parallel experiments where either HA was removed from the extracellular milieu or CD44 expression was knocked down, results demonstrate that HA-CD44 interactions promote cytostatic and cytotoxic resistance to treatment with carmustine or TMZ. In particular, resistance was robust compared to patient-

matched GS cultures, which we have previously shown do not express high levels of HA[21], underscoring the critical contributions of the local ECM microenvironment to GBM cell biology. Moreover, our results indicate that HA may promote GBM cell survival during treatment, allowing cells to recover during periods of “rest” from treatment, similar to a typical chemotherapy cycle in a clinical setting. Specifically, scaffolds with high HA content protected GBM cells from chemotherapy-induced apoptosis. HA may have a similar protective effect in clinical GBM, where increased HA expression positively correlates with tumor aggression [10,17],

Furthermore, we incorporated the integrin-binding, RGD tripeptide into HA hydrogel scaffolds to mimic interactions between cells and ECM proteins, many of which have been implicated in GBM aggression (e.g., collagen[49], fibronectin[50], and vitronectin[41]) and contain the RGD motif through which they can interact with integrin receptors[51]. An important design feature of the hydrogel scaffolds used here is that HA and RGD content can be varied independently of culture dimensionality, mechanical properties, and diffusivity[48]. Given that both integrin and CD44 receptors are mechano-responsive[8,20] and that mechanical properties of the 3D microenvironment have strong effects on treatment resistance in GBM[21,52], hydrogel mechanical properties were kept constant around 150 Pa (shear elastic modulus). Previously, we demonstrated that HA-rich hydrogels with this modulus maximized the ability of GBM cells to acquire resistance to targeted EGFR inhibition[21]. The differential effects of RGD when immobilized to insoluble hydrogel scaffolds, compared to when added as soluble cyclo-RGD (i.e., cilengitide), also provided evidence of force transduction from the matrix. Specifically, while immobilized RGD promoted resistance and an invasive morphology, these effects were reversed by addition of soluble RGD.

Consistent with our previous findings[21], increasing HA content in bioengineered matrices correlated with GBM cell upregulation in expression of the HA receptor CD44. Here, we demonstrate that engagement of CD44 and/or integrin αV induces downstream Src phosphorylation. In turn, activated Src suppressed expression of the BCL-2 family of pro-apoptotic factors in response to chemotherapies. When treated with alkylating chemotherapies — which function by damaging the DNA of rapidly dividing cells, such as cancer cells, to activate downstream apoptosis — this effect was more pronounced. Previous studies have reported that depressed apoptotic signaling in cancer cells may allow the cell to stay alive during an “intermediate” period over which they acquire resistance to treatment through other mechanisms, including repair of alkylated DNA through DNA mismatch repair (MMR) complexes and upregulation of drug efflux pumps such as p-glycoprotein[39]. Notably, we report the novel finding that ECM engagement rescues GBM cells from chemotherapy-induced apoptosis, potentially through suppression pro-apoptotic factors downstream of the P53 signaling pathway such as PUMA. This result suggests that treatment with a p53 activator, such as nutlin[25], in combination with alkylating chemotherapies may counteract the pro-survival actions of the tumor ECM.

Here, we found that addition of RGD to HA matrices reduced chemotherapy-induced apoptosis by around 50% (**Fig. 3B**) — consistent with previous findings in glioma and lung cancer models[41,42]. Furthermore, dual treatment of either chemotherapy with cilengitide, to disrupt integrin-RGD binding, resulted in around three-fold increase in cl-PARP expression over chemotherapy alone (**Fig. 3D**). We posit two potential explanations for these findings. First, it is likely that GBM cells deposited additional integrin-binding ECM proteins during the culture period and that cilengitide treatment inhibited these interactions as well as those with hydrogel-immobilized RGD, resulting in higher level of apoptosis. Second, disruption of integrin-RGD interactions may have interfered with chemo-protection provided by CD44-HA interactions, indicating the possibility of cooperative effects of CD44 and integrin αV signaling.

Observations of co-expression (**Fig. 4**) and systematic knockdowns (**Fig. 5**) of CD44 and integrin αV provided additional evidence that engagement of these two receptors within a 3D matrix acts cooperatively to protect GBM cells from drug-induced apoptosis. These results are in agreement with previous reports indicating that CD44 and integrins can physically interact at the cell membrane[6,34]. Furthermore, our results demonstrate that engagement of CD44 and integrin αV receptors amplified downstream activation of Src to suppress treatment-induced apoptosis (**Figs. 6, 7**). Previously, Src activation has been linked to integrin activation and invasive morphology[13,15,32], as well as survival and chemotherapy resistance[14,53], in various cancer types . However, to the best of our knowledge, this is the first report demonstrating a direct connection between interactions of CD44 and integrins with the 3D ECM leading to Src activation and downstream phenotypic changes in GBM cells. Our previous study demonstrated that HA and RGD present in 3D culture matrices could promote development of resistance to inhibition of using targeted treatments[21]. In this study, we revealed how the same matrix microenvironment intensifies Src activation, which others have reported to mediate resistance to EGFR inhibition via lapatinib in breast cancer[54]. Thus, we suspect that GBM may also be escape EGFR inhibition through matrix-mediated activation of Src.

While a previous phase II clinical trial (NCT00813943) found that addition of the integrin inhibitor cilengitide to radio- and chemotherapy improved median overall survival improved to 16.3 months from 13.4 months, the phase III trial did not find any improved outcomes (NCT00689221) [55,56]. Given our results showing the contribution of the non-integrin CD44 receptor to chemotherapy resistance, addition of therapies targeting the downstream signaling molecules of matrix-mediated resistance, such as Src, may be more beneficial. Although previous work has identified Src inhibition via dasatinib as a possibly effective monotherapy for treatment of GBM using standard, 2D cell culture experimental set-up[16], phase I/II clinical trials evaluating dasatinib for treatment of recurrent GBM found that dasatinib monotherapy was ineffective (NCT00423735)[57]. This result is consistent with our finding in 3D hydrogel cultures, where the response of GBM cells to dasatinib treatment alone was equivalent to vehicle controls (**Fig. 6F,G**), indicating that our novel hydrogel platform may be a better tool for *in vitro*, pre-clinical screening evaluation of therapeutic strategies than 2D culture methods. While dasatinib was not effective as a monotherapy, our results do indicate that dual treatment with dasatinib and chemotherapy may be effective. There has been one phase II clinical study that investigated the use of dasatinib treatment after the conclusion of more routine radiation and chemotherapy (TMZ) treatment in newly diagnosed GBM patients (NCT00869401). However, this study did not find any benefits of adding dasatinib over routine therapy alone. Our results indicate that dasatinib may only be effective if given in conjunction with, or even prior to, TMZ to inhibit Src activation and promote apoptosis. However, one cannot exclude other factors, such as inefficient penetration of dasatinib into patient tumors, as possible contributors to the clinical failure of dasatinib in GBM [58].

In conclusion, we report the use of a bioengineered, 3D culture platform to elucidate mechanisms underlying ECM-mediated chemotherapy resistance in patient-derived GBM cells. Our results demonstrate how matrix engagement of CD44 and integrin αV augments downstream Src activation, causing depression of BCL-2 family pro-apoptotic factors. This finding provides a strong rationale for investigating the efficacy of simultaneous treatment with Src inhibitors and TMZ in future studies.

Acknowledgements:

This work was supported with funding from the National Institutes of Health (NIH R21NS093199) and the UCLA Animal Resource Center (ARC) 3R's Award. A Dissertation Year Fellowship from UCLA Graduate Division provided support for W. Xiao and an NIH Training Grant in Genomic Analysis and Interpretation T32HG002536 provided support for J. Liang. Our sincerest thanks go to the lab of Dr. Harley Kornblum for provision of the HK301 cell line. We also thank UCLA Crump Institute for Molecular Imaging for using IVIS imaging system, UCLA Brain Research Institute (BRI) for use of the cryostat instrument, and the Flow Cytometry Core in Jonsson Comprehensive Cancer Center (JCCC) at UCLA for support and instrumentation for flow cytometry studies.

Author Contributions:

Concept and design: W. Xiao, D.A. Nathanson, S.K. Seidlits.

Development of methodology: W. Xiao, S. Wang, R. Zhang, A. Sohrabi, Q.Yu, S. Liu, A. Ehsanipour, J. Liang.

Acquisition and analysis of data: W. Xiao, S. Wang, R. Zhang, S. Liu,

Write, review and/or revision of the manuscript: W. Xiao, A. Ehsanipour, J. Liang, R.D. Bierman, D.A. Nathanson, S.K. Seidlits.

Study supervision: D.A. Nathanson, S.K. Seidlits.

References:

[1] E.C. Holland, Glioblastoma multiforme: The terminator, Proc. Natl. Acad. Sci. 97 (2000) 6242–6244. doi:10.1073/pnas.97.12.6242.

[2] Q.T. Ostrom, H. Gittleman, P. Farah, A. Ondracek, Y. Chen, Y. Wolinsky, N.E. Stroup, C. Kruchko, J.S. Barnholtz-sloan, CBTRUS statistical report: Primary brain and central nervous system tumors diagnosed in the United States in 2006 - 2010, J. Neurooncol. 15 (2013) 788–796. doi:10.1093/neuonc/not151.

[3] R. Stupp, W. Mason, M.J. van den Bent, M. Weller, B.M. Fisher, M.J.B. Taphoorn, K. Belanger, A.A. Brandes, C. Marosi, U. Bogdahn, J. Curschmann, R.C. Janzer, S.K. Ludwin, T. Gorlia, A. Allgeier, D. Lacombe, G. Cairncross, E. Eisenhauer, R.O. Mirimanoff, Radiotherapy plus Concomitant\nand Adjuvant Temozolomide for Glioblastoma, N. Engl. J. Med. (2005). doi:10.1056/NEJMoa043330.

[4] S.J. Wang, L.Y.W. Bourguignon, Hyaluronan and the interaction between CD44 and epidermal growth factor receptor in oncogenic signaling and chemotherapy resistance in head and neck cancer, Arch. Otolaryngol. Neck Surg. 132 (2006) 771–778. doi:10.1001/archotol.132.7.771.

[5] L.Y.W. Bourguignon, Z. Hongbo, L. Shao, Y.W. Chen, CD44 interaction with Tiam1 promotes Rac1 signaling and hyaluronic acid- mediated breast tumor cell migration, J. Biol. Chem. 275 (2000) 1829–1838. doi:10.1074/jbc.275.3.1829.

[6] H. Ponta, L. Sherman, P.A. Herrlich, CD44: From adhesion molecules to signalling regulators, Nat. Rev. Mol. Cell Biol. 4 (2003) 33. doi:10.1038/nrm1004.

[7] W. Guo, F.G. Giancotti, Integrin signalling during tumour progression, Nat. Rev. Mol. Cell Biol. 5 (2004) 816–826. doi:10.1038/nrm1490.

[8] Y. Kim, S. Kumar, CD44-Mediated Adhesion to Hyaluronic Acid Contributes to

Mechanosensing and Invasive Motility, Mol. Cancer Res. 12 (2014) 1416–1429. doi:10.1158/1541-7786.MCR-13-0629.

[9] L. Jadin, S. Pastorino, R. Symons, N. Nomura, P. Jiang, T. Juarez, M. Makale, S. Kesari, Hyaluronan expression in primary and secondary brain tumors, Ann. Transl. Med. 3 (2015) 80. doi:10.3978/j.issn.2305-5839.2015.04.07.

[10] J.B. Park, H.-J.J. Kwak, S.-H.H. Lee, Role of hyaluronan in glioma invasion, Cell Adh. Migr. 2 (2008) 202–207. doi:10.4161/cam.2.3.6320.

[11] M.P. Playford, M.D. Schaller, The interplay between Src and integrins in normal and tumor biology, Oncogene. 23 (2004) 7928. doi:10.1038/sj.onc.1208080.

[12] S.K. Mitra, D.D. Schlaepfer, Integrin-regulated FAK-Src signaling in normal and cancer cells, Curr. Opin. Cell Biol. 18 (2006) 516–523. doi:10.1016/j.ceb.2006.08.011.

[13] L.Y.W. Bourguignon, H. Zhu, L. Shao, Y.-W. Chen, CD44 interaction with c-Src kinase promotes cortactin-mediated cytoskeleton function and hyaluronic acid-dependent ovarian tumor cell migration, J. Biol. Chem. 276 (2001) 7327–7336.

[14] Q. Guo, L. Lu, Y. Liao, X. Wang, Y. Zhang, Y. Liu, S. Huang, H. Sun, Z. Li, L. Zhao, Influence of c-Src on hypoxic resistance to paclitaxel in human ovarian cancer cells and reversal of FV-429, Cell Death Dis. 8 (2018) e3178. doi:10.1038/cddis.2017.367.

[15] A.C. Shor, E.A. Keschman, F.Y. Lee, C. Muro-Cacho, G.D. Letson, J.C. Trent, W.J. Pledger, R. Jove, Dasatinib inhibits migration and invasion in diverse human sarcoma cell lines and induces apoptosis in bone sarcoma cells dependent on Src kinase for survival, Cancer Res. 67 (2007) 2800–2808. doi:10.1158/0008-5472.CAN-06-3469.

[16] J. Du, P. Bernasconi, K.R. Clauser, D.R. Mani, S.P. Finn, R. Beroukhim, M. Burns, B. Julian, X.P. Peng, H. Hieronymus, R.L. Maglathlin, T.A. Lewis, L.M. Liau, P. Nghiemphu, I.K. Mellinghoff, D.N. Louis, M. Loda, S.A. Carr, A.L. Kung, T.R. Golub, Bead-based profiling of tyrosine kinase phosphorylation identifies SRC as a potential target for glioblastoma therapy, Nat. Biotechnol. 27 (2009) 77. doi:10.1038/nbt.1513.

[17] W. Xiao, A. Sohrabi, S.K. Seidlits, Integrating the glioblastoma microenvironment into engineered experimental models, Futur. Sci. OA. 3 (2017) FSO189. doi:10.4155/fsoa-2016-0094.

[18] W. Norde, Adsorption of proteins from solution at the solid-liquid interface, Adv. Colloid Interface Sci. 25 (1986) 267–340. doi:10.1016/0001-8686(86)80012-4.

[19] J. Lee, S. Kotliarova, Y. Kotliarov, A. Li, Q. Su, N.M. Donin, S. Pastorino, B.W. Purow, N. Christopher, W. Zhang, Tumor stem cells derived from glioblastomas cultured in bFGF and EGF more closely mirror the phenotype and genotype of primary tumors than do serum-cultured cell lines, Cancer Cell. 9 (2006) 391–403. doi:10.1016/j.ccr.2006.03.030.

[20] A. Katsumi, A.W. Orr, E. Tzima, M.A. Schwartz, Integrins in Mechanotransduction, J. Biol. Chem. 279 (2004) 12001–12004. doi:10.1074/jbc.R300038200.

[21] W. Xiao, R. Zhang, A. Sohrabi, A. Ehsanipour, S. Sun, J. Liang, C. Walthers, L. Ta, D.A. Nathanson, S.K. Seidlits, Brain-Mimetic 3D Culture Platforms Allow Investigation of Cooperative Effects of Extracellular Matrix Features on Therapeutic Resistance in Glioblastoma, Cancer Res. 78 (2018) 1358–1370. doi:10.1158/0008-5472.CAN-17-2429.

[22] W. Xiao, A. Ehsanipour, A. Sohrabi, S.K. Seidlits, Hyaluronic-Acid Based Hydrogels for 3-

Dimensional Culture of Patient-Derived Glioblastoma Cells, J. Vis. Exp. (2018) e58176. doi:10.3791/58176.

[23] J.N. Sarkaria, B.L. Carlson, M.A. Schroeder, P. Grogan, P.D. Brown, C. Giannini, K. Ballman, G.J. Kitange, A. Guha, A. Pandita, C.D. James, Use of an Orthotopic Xenograft Model for Assessing the Effect of Epidermal Growth Factor Receptor Amplification on Glioblastoma Radiation Response Cancer Therapy : Preclinical Epidermal Growth Factor Receptor Amplification on Glioblastoma Radiation Respon, Clin. Cancer Res. 12 (2006) 2264–71. doi:10.1158/1078-0432.CCR-05-2510.

[24] D.R. Laks, T.J. Crisman, M. Shih, J. Mottahedeh, F. Gao, J. Sperry, M.C. Garrett, W.H. Yong, T.F. Cloughesy, L.M. Liau, Large-scale assessment of the gliomasphere model system, Neuro. Oncol. 18 (2016) 1367–1378. doi:10.1093/neuonc/now045.

[25] W.X. Mai, L. Gosa, V.W. Daniels, L. Ta, J.E. Tsang, B. Higgins, W.B. Gilmore, N.A. Bayley, M.D. Harati, J.T. Lee, W.H. Yong, H.I. Kornblum, S.J. Bensinger, P.S. Mischel, P.N. Rao, P.M. Clark, T.F. Cloughesy, A. Letai, D.A. Nathanson, Cytoplasmic p53 couples oncogene-driven glucose metabolism to apoptosis and is a therapeutic target in glioblastoma, Nat. Med. (2017) 1342–1351. doi:10.1038/nm.4418.

[26] T. Dull, R. Zufferey, M. Kelly, R.J. Mandel, M. Nguyen, D. Trono, L. Naldini, A third-generation lentivirus vector with a conditional packaging system, J. Virol. 72 (1998) 8463–8471.

[27] R. Stupp, W. Mason, M.J. van den Bent, M. Weller, B.M. Fisher, M.J.B. Taphoorn, K. Belanger, A.A. Brandes, C. Marosi, U. Bogdahn, J. Curschmann, R.C. Janzer, S.K. Ludwin, T. Gorlia, A. Allgeier, D. Lacombe, G. Cairncross, E. Eisenhauer, R.O. Mirimanoff, Radiotherapy plus Concomitant and Adjuvant Temozolomide for Glioblastoma, New Engl. J. Med. 352 (2005) 987–996. doi:10.1056/NEJMoa043330.

[28] S.Y. Lee, Temozolomide resistance in glioblastoma multiforme, Genes Dis. 3 (2016) 198–210. doi:10.1016/j.gendis.2016.04.007.

[29] A.C. Bellail, S.B. Hunter, D.J. Brat, C. Tan, E.G. Van Meir, Microregional extracellular matrix heterogeneity in brain modulates glioma cell invasion, Int. J. Biochem. Cell Biol. 36 (2004) 1046–1069. doi:10.1016/j.biocel.2004.01.013.

[30] D.A. Reardon, B. Neyns, M. Weller, J.C. Tonn, L.B. Nabors, R. Stupp, Cilengitide: an RGD pentapeptide αvβ3 and αvβ5 integrin inhibitor in development for glioblastoma and other malignancies, Futur. Oncol. 7 (2011) 339–354. doi:10.2217/fon.11.8.

[31] M.C. Chamberlain, T. Cloughsey, D.A. Reardon, P.Y. Wen, A novel treatment for glioblastoma: integrin inhibition, Expert Rev. Neurother. 12 (2012) 421–435. doi:10.1586/ern.11.188.

[32] D. Huveldt, L.J. Lewis-Tuffin, B.L. Carlson, M.A. Schroeder, F. Rodriguez, C. Giannini, E. Galanis, J.N. Sarkaria, P.Z. Anastasiadis, Targeting Src Family Kinases Inhibits Bevacizumab-Induced Glioma Cell Invasion, PLoS One. (2013). doi:10.1371/journal.pone.0056505.

[33] M.S. Ahluwalia, J. de Groot, W.M. Liu, C.L. Gladson, Targeting SRC in glioblastoma tumors and brain metastases: Rationale and preclinical studies, Cancer Lett. 298 (2010) 139–149. doi:10.1016/j.canlet.2010.08.014.

[34] T. Fujisaki, Y. Tanaka, K. Fujii, S. Mine, K. Saito, S. Yamada, U. Yamashita, T. Irimura, S.

Eto, CD44 stimulation induces integrin-mediated adhesion of colon cancer cell lines to endothelial cells by up-regulation of integrins and c-Met and activation of integrins, Cancer Res. 59 (1999) 4427–4434.

[35] K. V. Lu, S. Zhu, A. Cvrljevic, T.T. Huang, S. Sarkaria, D. Ahkavan, J. Dang, E.B. Dinca, S.B. Plaisier, I. Oderberg, Y. Lee, Z. Chen, J.S. Caldwell, Y. Xie, J.A. Loo, D. Seligson, A. Chakravari, F.Y. Lee, R. Weinmann, T.F. Cloughesy, S.F. Nelson, G. Bergers, T. Graeber, F.B. Furnari, C.D. James, W.K. Cavenee, T.G. Johns, P.S. Mischel, Fyn and Src Are Effectors of Oncogenic Epidermal Growth Factor Receptor Signaling in Glioblastoma Patients, Cancer Res. 69 (2009) 6889–6898. doi:10.1158/0008-5472.CAN-09-0347.

[36] R. Karni, R. Jove, A. Levitzki, Inhibition of pp60(c-Src) reduces Bcl-X(L) expression and reverses the transformed phenotype of cells overexpressing EGF and HER-2 receptors, Oncogene. 18 (1999) 4654. doi:10.1038/sj.onc.1202835.

[37] S. Bhattacharya, R.M. Ray, L.R. Johnson, Integrin beta3-mediated Src activation regulates apoptosis in IEC-6 cells via Akt and STAT3, Biochem. J. 397 (2006) 437–447. doi:10.1042/BJ20060256.

[38] J.M. Adams, S. Cory, The Bcl-2 apoptotic switch in cancer development and therapy, Oncogene. 26 (2007) 1324. doi:10.1038/sj.onc.1210220.

[39] G. Perazzoli, J. Prados, R. Ortiz, O. Caba, L. Cabeza, M. Berdasco, B. Gónzalez, C. Melguizo, Temozolomide resistance in glioblastoma cell lines: Implication of MGMT, MMR, P-glycoprotein and CD133 expression, PLoS One. 10 (2015). doi:10.1371/journal.pone.0140131.

[40] P.J. Morin, Drug resistance and the microenvironment: Nature and nurture, Drug Resist. Updat. 6 (2003) 169–172. doi:10.1016/S1368-7646(03)00059-1.

[41] J.H. Uhm, N.P. Dooley, A.P. Kyritsis, J.S. Rao, C.L. Gladson, Vitronectin, a glioma-derived extracellular matrix protein, protects tumor cells from apoptotic death., Clin. Cancer Res. 5 (1999) 1587–1594. doi:10.3171/jns.1986.65.5.0654.

[42] T. Sethi, R.C. Rintoul, S.M. Moore, a C. MacKinnon, D. Salter, C. Choo, E.R. Chilvers, I. Dransfield, S.C. Donnelly, R. Strieter, C. Haslett, Extracellular matrix proteins protect small cell lung cancer cells against apoptosis: a mechanism for small cell lung cancer growth and drug resistance in vivo., Nat. Med. 5 (1999) 662. doi:10.1038/9511.

[43] S.J. Florczyk, K. Wang, S. Jana, D.L. Wood, S.K. Sytsma, J.G. Sham, F.M. Kievit, M. Zhang, Porous chitosan-hyaluronic acid scaffolds as a mimic of glioblastoma microenvironment ECM, Biomaterials. 34 (2013) 10143–10150. doi:10.1016/j.biomaterials.2013.09.034.

[44] C.J. Jiglaire, N. Baeza-Kallee, E. Denicolaï, D. Barets, P. Metellus, L. Padovani, O. Chinot, D. Figarella-Branger, C. Fernandez, C. Jiguet Jiglaire, N. Baeza-Kallee, E. Denicolaï, D. Barets, P. Metellus, L. Padovani, O. Chinot, D. Figarella-Branger, C. Fernandez, Ex vivo cultures of glioblastoma in three-dimensional hydrogel maintain the original tumor growth behavior and are suitable for preclinical drug and radiation sensitivity screening, Exp. Cell Res. 321 (2014) 99–108. doi:10.1016/j.yexcr.2013.12.010.

[45] S. Pedron, H. Polishetty, A.M. Pritchard, B.P. Mahadik, J.N. Sarkaria, B.A.C. Harley, Spatially graded hydrogels for preclinical testing of glioblastoma anticancer therapeutics, MRS Commun. 7 (2017) 442–449. doi:10.1557/mrc.2017.85.

[46] R. Edmondson, J.J. Broglie, A.F. Adcock, L. Yang, Three-Dimensional Cell Culture Systems and Their Applications in Drug Discovery and Cell-Based Biosensors, Assay Drug Dev. Technol. 12 (2014) 207–218. doi:10.1089/adt.2014.573.

[47] M. Ravi, V. Paramesh, S.R. Kaviya, E. Anuradha, F.D. Paul Solomon, 3D cell culture systems: Advantages and applications, J. Cell. Physiol. 230 (2015) 16–26. doi:10.1002/jcp.24683.

[48] K. Wang, F.M. Kievit, A.E. Erickson, J.R. Silber, R.G. Ellenbogen, M. Zhang, Culture on 3D Chitosan-Hyaluronic Acid Scaffolds Enhances Stem Cell Marker Expression and Drug Resistance in Human Glioblastoma Cancer Stem Cells, Adv. Healthc. Mater. 5 (2016) 3173–3181. doi:10.1002/adhm.201600684.

[49] T. Mammoto, A. Jiang, E. Jiang, D. Panigrahy, M.W. Kieran, A. Mammoto, Role of Collagen Matrix in Tumor Angiogenesis and Glioblastoma Multiforme Progression, Am. J. Pathol. 183 (2013) 1293–1305. doi:10.1016/j.ajpath.2013.06.026.

[50] E. Serres, F. Debarbieux, F. Stanchi, L. Maggiorella, D. Grall, L. Turchi, F. Burel-Vandenbos, D. Figarella-Branger, T. Virolle, G. Rougon, E. Van Obberghen-Schilling, Fibronectin expression in glioblastomas promotes cell cohesion, collective invasion of basement membrane in vitro and orthotopic tumor growth in mice, Br. Dent. J. (2014). doi:10.1038/onc.2013.305.

[51] S.K. Akiyama, K. Olden, K.M. Yamada, Fibronectin and integrins in invasion and metastasis, Cancer Metastasis Rev. 14 (1995) 173–189. doi:10.1007/BF00690290.

[52] C.R.I. Lam, H.K. Wong, S. Nai, C.K. Chua, N.S. Tan, L.P. Tan, A 3D biomimetic model of tissue stiffness interface for cancer drug testing, Mol. Pharm. (2014). doi:10.1021/mp500059q.

[53] J.-L. Lee, M.-J. Wang, P.-R. Sudhir, J.-Y. Chen, CD44 engagement promotes matrix-derived survival through the CD44-SRC-integrin axis in lipid rafts, Mol. Cell. Biol. 28 (2008) 5710–5723. doi:10.1128/MCB.00186-08.

[54] L. Formisano, L. Nappi, R. Rosa, R. Marciano, C. D'Amato, V. D'Amato, V. Damiano, L. Raimondo, F. Iommelli, A. Scorziello, G. Troncone, B.M. Veneziani, S.J. Parsons, S. De Placido, R. Bianco, Epidermal growth factor-receptor activation modulates Src-dependent resistance to lapatinib in breast cancer models, Breast Cancer Res. 16 (2014) R45. doi:10.1186/bcr3650.

[55] R. Stupp, M.E. Hegi, T. Gorlia, S.C. Erridge, J. Perry, Y.-K. Hong, K.D. Aldape, B. Lhermitte, T. Pietsch, D. Grujicic, Cilengitide combined with standard treatment for patients with newly diagnosed glioblastoma with methylated MGMT promoter (CENTRIC EORTC 26071-22072 study): a multicentre, randomised, open-label, phase 3 trial, Lancet Oncol. 15 (2014) 1100–1108. doi:10.1016/S1470-2045(14)70379-1.

[56] L.B. Nabors, K.L. Fink, T. Mikkelsen, D. Grujicic, R. Tarnawski, D.H. Nam, M. Mazurkiewicz, M. Salacz, L. Ashby, V. Zagonel, R. Depenni, J.R. Perry, C. Hicking, M. Picard, M.E. Hegi, B. Lhermitte, D.A. Reardon, Two cilengitide regimens in combination with standard treatment for patients with newly diagnosed glioblastoma and unmethylated MGMT gene promoter: Results of the open-label, controlled, randomized phase II CORE study, Neuro. Oncol. 17 (2015) 708–717. doi:10.1093/neuonc/nou356.

[57] A.B. Lassman, S.L. Pugh, M.R. Gilbert, K.D. Aldape, S. Geinoz, J.H. Beumer, S.M. Christner, R. Komaki, L.M. Deangelis, R. Gaur, E. Youssef, H. Wagner, M. Won, M.P.

Mehta, Phase 2 trial of dasatinib in target-selected patients with recurrent glioblastoma (RTOG 0627), Neuro. Oncol. 17 (2015) 992–998. doi:10.1093/neuonc/nov011.

[58] S. Agarwal, R.K. Mittapalli, D.M. Zellmer, J.L. Gallardo, R. Donelson, C. Seiler, S.A. Decker, K.S. Santacruz, J.L. Pokorny, J.N. Sarkaria, W.F. Elmquist, J.R. Ohlfest, Active efflux of Dasatinib from the brain limits efficacy against murine glioblastoma: broad implications for the clinical use of molecularly targeted agents., Mol. Cancer Ther. 11 (2012) 2183–92. doi:10.1158/1535-7163.MCT-12-0552.

Figure Captions

Figure 1. High HA content hydrogels facilitate chemotherapy resistance. A) Schematic of 12-day chemotherapy treatment regimen consisting of 2 cycles of 3 days of treatment followed by 3 days of “rest”. Drug treatments included carmustine, temozolomide (TMZ), or vehicle (ethanol for carmustine, DMSO for TMZ). B) Representative phase contrast image of HK301 cells cultured in 3D scaffolds with low (0.1% w/v) or high (0.5% w/v) hyaluronic acid (HA) after the 12-day drug treatment. Scale bars = 200 μm. C) Representative bioluminescence measurements (single biological repeat shown) of HK301 cells over 12 days of treatment. Relative luminescence units (RLU) was normalized for background and measurement area. Within each condition, normalized RLU of treated samples were normalized to vehicle controls at each time point, then to signal before treatment (day 0). Two-way ANOVA (culture condition, time) was performed. Error bars show standard deviations (n=3). D) Bioluminescence signal in treated cultures of HK301 and GBM6 cells normalized to vehicle controls at the end of the 12-day chemotherapy regimen (n=3). One-way ANOVA followed by Tukey’s multiple comparison tests were performed. Error bars show standard deviations. *p<0.5, **p<0.01, ***p<0.001, ****p<0.0001, “ns” represents non-significance.

Figure 2. Hyaluronic acid (HA) in 3D matrices interacts with CD44 to protect against chemotherapy-induced apoptosis. A) Representative flow cytometry plots showing EdU+ GBM6 cells (EdU incorporation by cells undergoing division, through S-phase, during a 2.5 hr incubation) after 3 days of carmustine treatment (100 μM). B) Representative Western blots showing cl-PARP expression in HK301 cells cultured in high HA (0.5% w/v) matrices or as gliomaspheres (GS) after 3 days of carmustine (50 μM) or TMZ (500 μM) treatment. C) Left panel: Representative Western blots showing cl-PARP expression in GBM6 cells cultured in matrices with low (0.1 w/v) or high (0.5% w/v) HA after 3 days of treatment with carmustine (Carm., 100 μM), temozolomide (TMZ, 500 μM), or vehicle. Right panel: Densitometry analysis of Western blots, cl-PARP normalized to GAPDH, across independent repeats (n=3). D) Left panel: Representative Western blots showing cl-PARP expression in GBM6 cells (wildtype and shRNA knockdown of CD44) cultured in high HA matrices after 3 days of treatment with carmustine (Carm., 100 μM), temozolomide (TMZ, 500 μM), or vehicle. Right panel: Densitometry analysis of Western blots, cl-PARP normalized to GAPDH, across independent repeats (n=3). C, D) Error bars show standard deviations. A student’s t test was used to compare cl-PARP expression within each treatment arm. *p<0.5, **p<0.01, ***p<0.001, ****p<0.0001, “ns” represents non-significance.

Figure 3. Hyaluronic acid (HA) and RGD synergistically protect against treatment-induced apoptosis. A) Representative phase contrast images of HK301 cells cultured for 8 days in hydrogels with high HA (0.5% w/v) and either adhesive peptides bearing the RGD motif or non-adhesive cysteines ("CYS") as a negative control. Arrows indicate cells displaying invasive morphologies. Scale bars = 200 µm. B) Upper panel: Representative Western blots showing cl-PARP expression in HK301 cells, cultured in high HA matrices containing RGD (or CYS control) peptides, after 3 days of treatment with carmustine (Carm., 50 µM), temozolomide (TMZ, 500 µM), or vehicle. Lower panel: Densitometry analysis of Western blots, cl-PARP normalized to GAPDH, across independent repeats (n=3). C) Representative phase contrast images of HK301 cells cultured in 3D hydrogel matrices with high HA and RGD after 4 days after cilengitide treatment (50 µM). Cells were cultured for 8 days in hydrogels before starting cilengitide treatment. Arrows indicate cells displaying invasive morphologies. Scale bars = 200 µm. D) Upper panel: Representative Western blots showing cl-PARP expression in GBM6 cells cultured in 3D hydrogel matrices with high HA and RGD after 3 days of treatment with carmustine (Carm., 100 µM), temozolomide (TMZ, 500 µM), or vehicle. Cilengitide treatment (50 µM) was started 4 days before beginning chemotherapy treatment. Lower panel: Densitometry analysis of Western blots, cl-PARP normalized to GAPDH, across independent repeats (n=3). Two-way ANOVA (cilengitide, chemotherapy) was performed. p_{int}= 0.03 for HK301 and p_{int}=0.005 for GBM6. Error bars show standard deviations. A student's t-test was used to compare cl-PARP expression within each treatment arm. *p<0.5, **p<0.01, ***p<0.001, ****p<0.0001, "ns" represents non-significance.

Figure 4. CD44 and Integrin αV are co-expressed by GBM cells cultured in 3D matrices containing both hyaluronic acid (HA) and RGD peptides. Representative fluorescence images of immunostaining for CD44 (red) and integrin αV (green) of GBM6 and HK301 cells cultured in high HA matrices containing RGD (or CYS control) peptide for 8 days. Nuclei were counterstained with Hoescht 33342 (blue). Primary antibody was omitted for negative control images. Arrows indicate areas of CD44 and integrin αV co-expression (yellow). Cells were cultured 8 days before cilengitide treatment (50 µM), which continued for 3 days. Scale bars = 200 µm (20 µm for magnified insets of areas shown by white boxes).

Figure 5. Integrin αV and CD44 mediate both chemotherapy resistance and invasive morphology cultured in 3D matrices including hyaluronic acid (HA) and RGD motifs. A) Representative phase contrast images of HK301 cells (wildtype and shRNA knockdowns of CD44 and/or integrin αV (ITGAV)) cultured for 8 days in hydrogels with high HA and RGD. Arrows indicate cells displaying invasive morphologies. Areas indicated by white boxes in the top row of images are shown at higher magnification in the bottom row. Scale bars = 200 µm. B) Left panel: Representative Western blots showing cl-PARP expression in HK301 cells (wildtype and shRNA knockdown of ITGAV) cultured in hydrogels with high HA and RGD after 3 days of treatment with with carmustine (Carm., 50 µM), temozolomide (TMZ, 500 µM), or vehicle. Right panel: Densitometry analysis of Western blots, cl-PARP normalized to GAPDH, across independent repeats (n=3). A student's t test was performed to compare cl-PARP expression within each treatment arm. Error bars show standard deviations. C) Left panel: Representative bioluminescence signal overlaid with a photograph of HK301 cultures on the 12th day 12 of chemotherapy treatment regimen. Red circles indicate locations of hydrogel cultures with the

well plate. Right panel: Bioluminescence signal (RLU – Relative Luminescence Units) in treated cultures of HK301 cells normalized to vehicle controls at the end of the 12-day chemotherapy regimen (n=3). One-way ANOVA with Tukey's multiple comparison tests was performed. Error bars show standard deviations. ****p<0.0001.

Figure 6. HA-CD44 and RGD-integrin αV interactions promote chemotherapy resistance through Src signaling. A-D) Representative Western blots showing Src phosphorylation in GBM cells (HK301, GBM6, GS024, GS025 lines). For A, C and D, cell lysates were collected after 8 days in 3D culture. For B, cilengitide (50 µM) treatment was started on day 8 of culture and cell lysates were collected after 3 days of treatment. Densitometry analysis showing the ratio of p-SRC to t-SRC is indicated within each panel. E) Representative phase contrast images of HK301 cells cultured in hydrogel matrices with high HA (0.5% v/w) and RGD for 4 days, then treated for 4 days with dasatinib (100 nM) or vehicle (DMSO). Arrows show cells displaying invasive morphologies. Scale bars = 200 µm. F) Upper panel: Representative Western blots showing Src phosphorylation in GBM6 after 3 days of treatment with carmustine (Carm., 100 µM), temozolomide (TMZ, 500 µM), or vehicle. Dasatinib (100 nM) or vehicle (DMSO) was started 4 days before adding chemotherapy treatment. Lower panel: Densitometry analysis of Western blots, cl-PARP normalized to GAPDH, across independent repeats (n=3). Student's t test was performed to compare cl-PARP expression within each treatment arm. Error bars show standard deviations. Two-way ANOVA (dasatinib, chemotherapy) was performed. p_{int}= 0.003 for HK301 and p_{int}=0.0002 for GBM6. G) Left panel: Representative bioluminescence signal overlaid with a photograph of HK301 cultures on the 12th day 12 of chemotherapy treatment regimen. Red circles indicate locations of hydrogel cultures with the well plate. Right panel: Bioluminescence signal in treated cultures of HK301 cells normalized to vehicle controls at the end of the 12-day chemotherapy regimen (n=3). Two-way ANOVA (dasatinib, chemotherapy) was performed. p_{int}= 0.03. Error bars show standard deviations. *p<0.5, **p<0.01, ***p<0.001, ****p<0.0001, "ns" represents non-significance.

Figure 7. Hydrogel matrices containing HA and RGD adhesive peptides protect 3D-cultured GBM cells from drug-induced apoptosis through suppression of PUMA, BAK and BAX. A-E) Representative Western blots showing expression of BCL-2 family factors, PUMA, BAK and BAX, in HK301 cells. For A-D, cells were culture in 0.5% HA (w/v) hydrogels with RGD peptides. For E, no RGD was added to hydrogels. Blots were performed on cell lysates collected after 3 days of treatment with chemotherapy or vehicle. Densitometry analysis of integrated band intensities normalized to GAPDH is indicated in each panel. Please see Figure S7 for statistical summarization of the western blotting experiments.

Figure 1

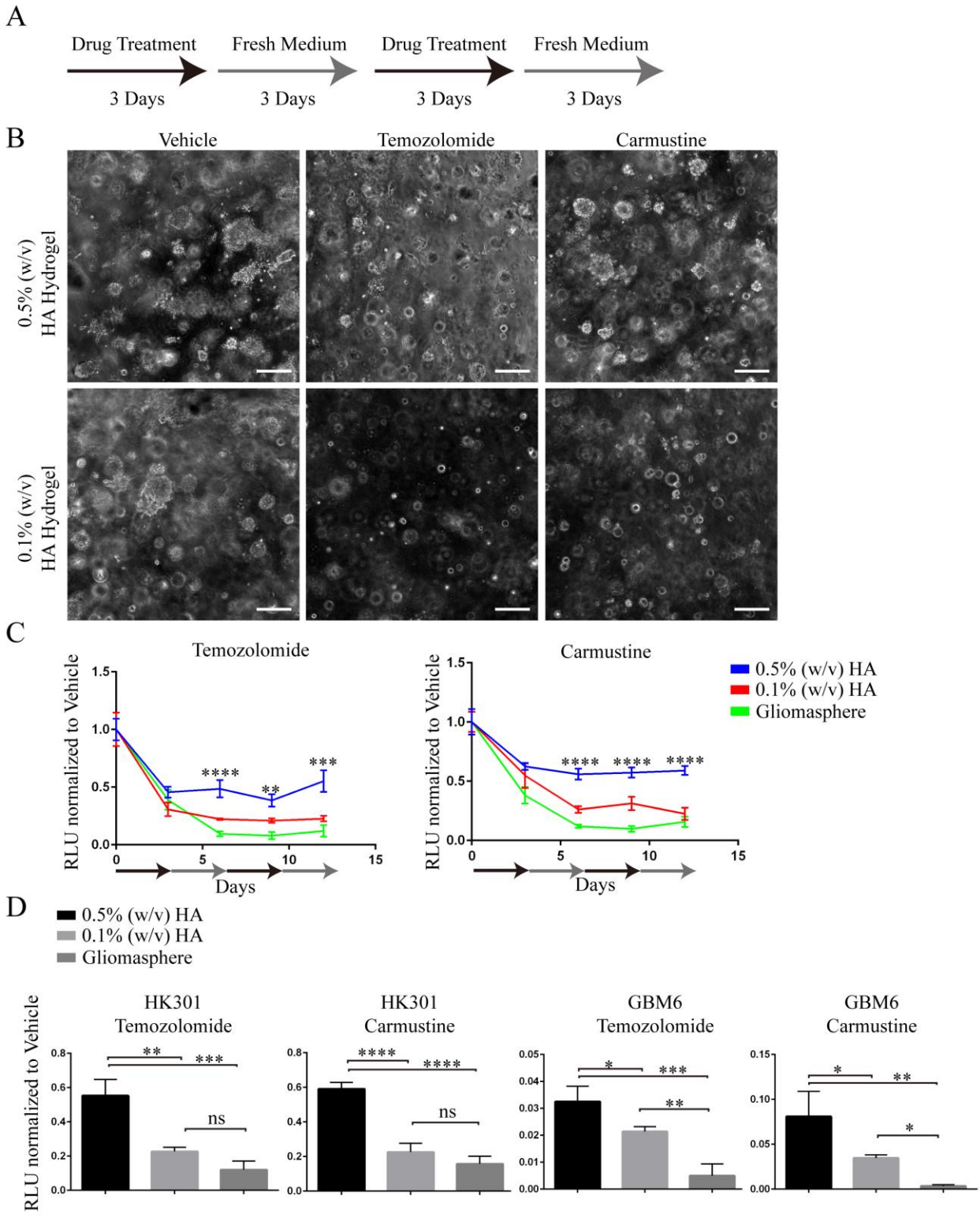

Figure 2

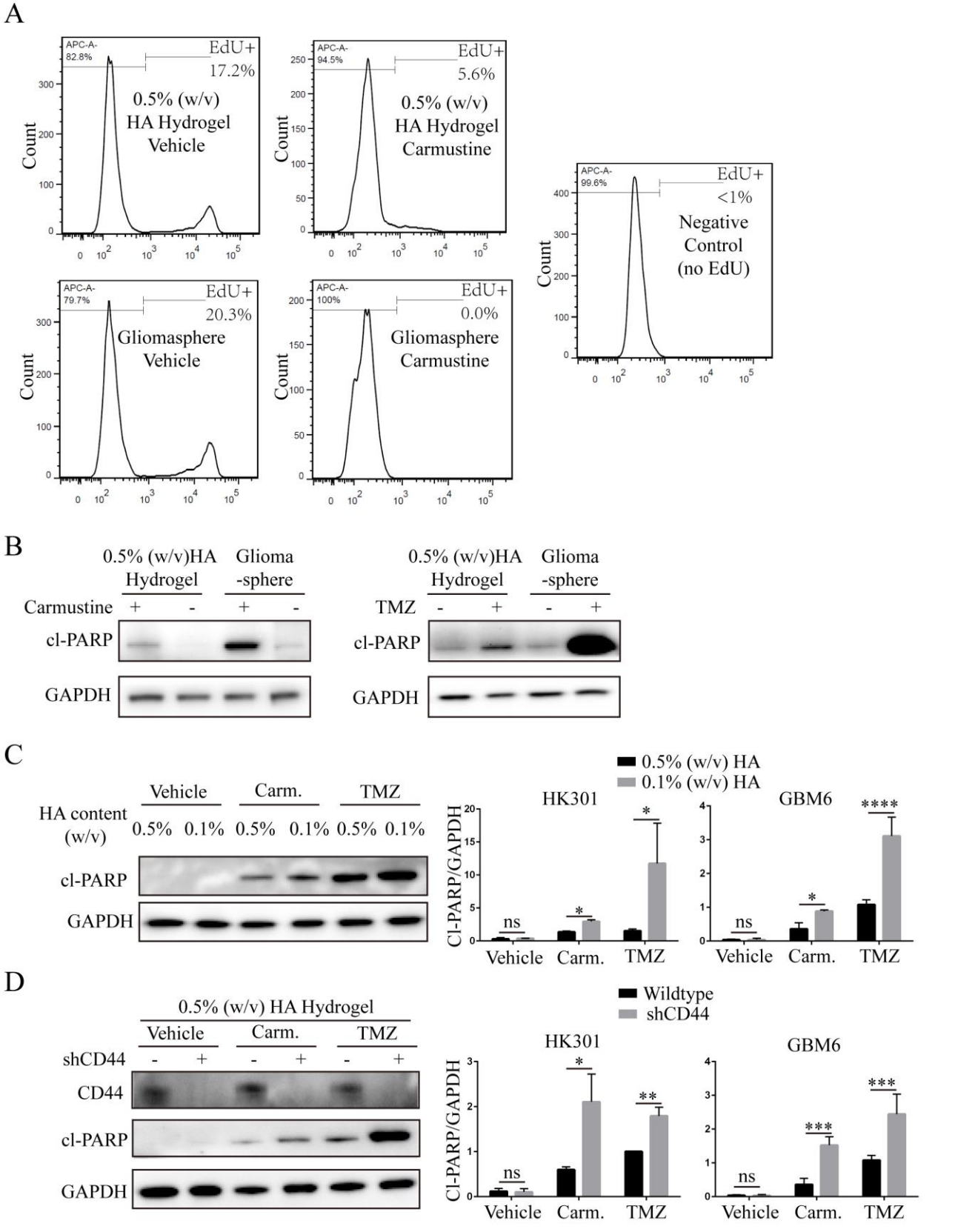

Figure 3

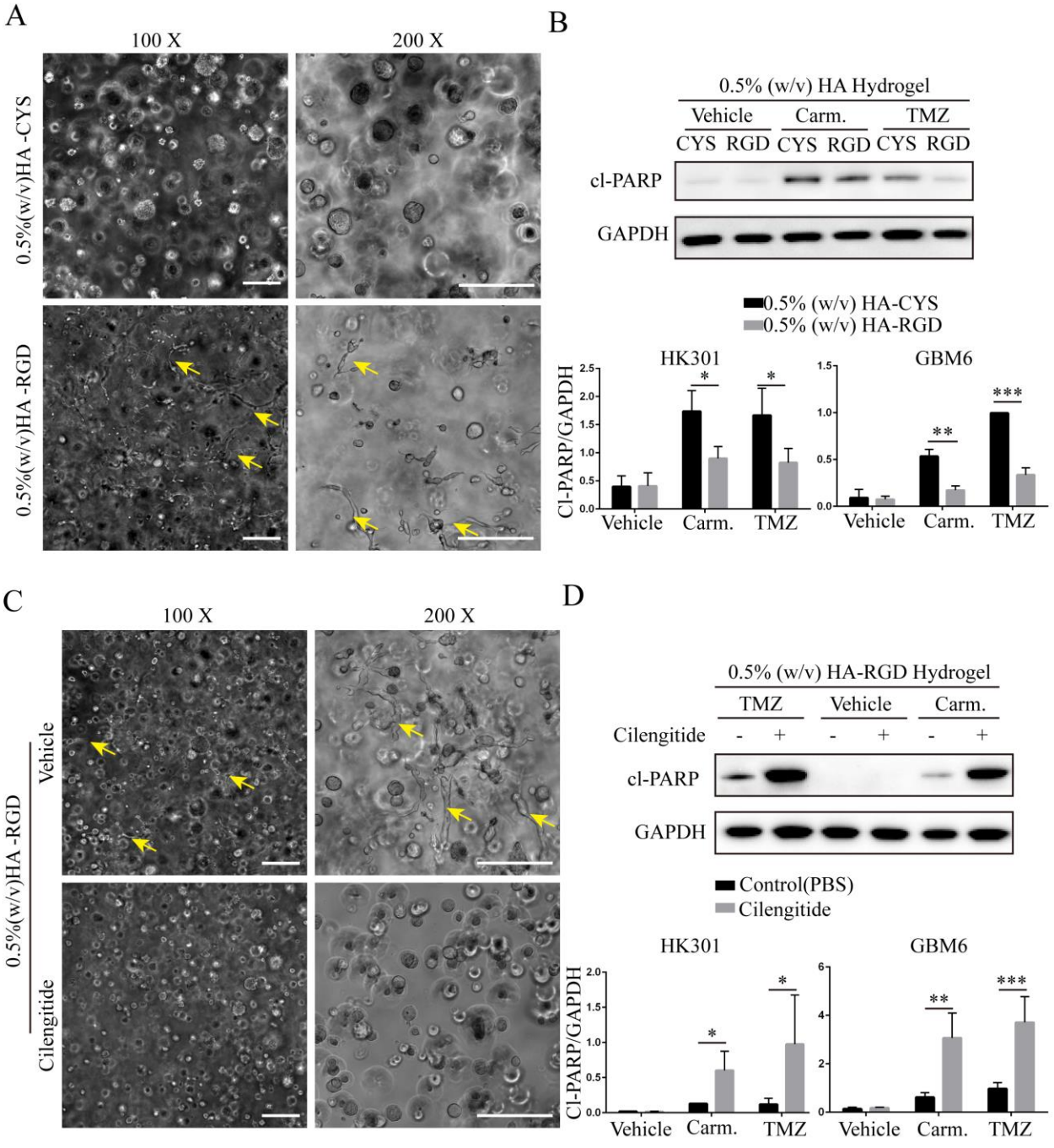

Figure 4

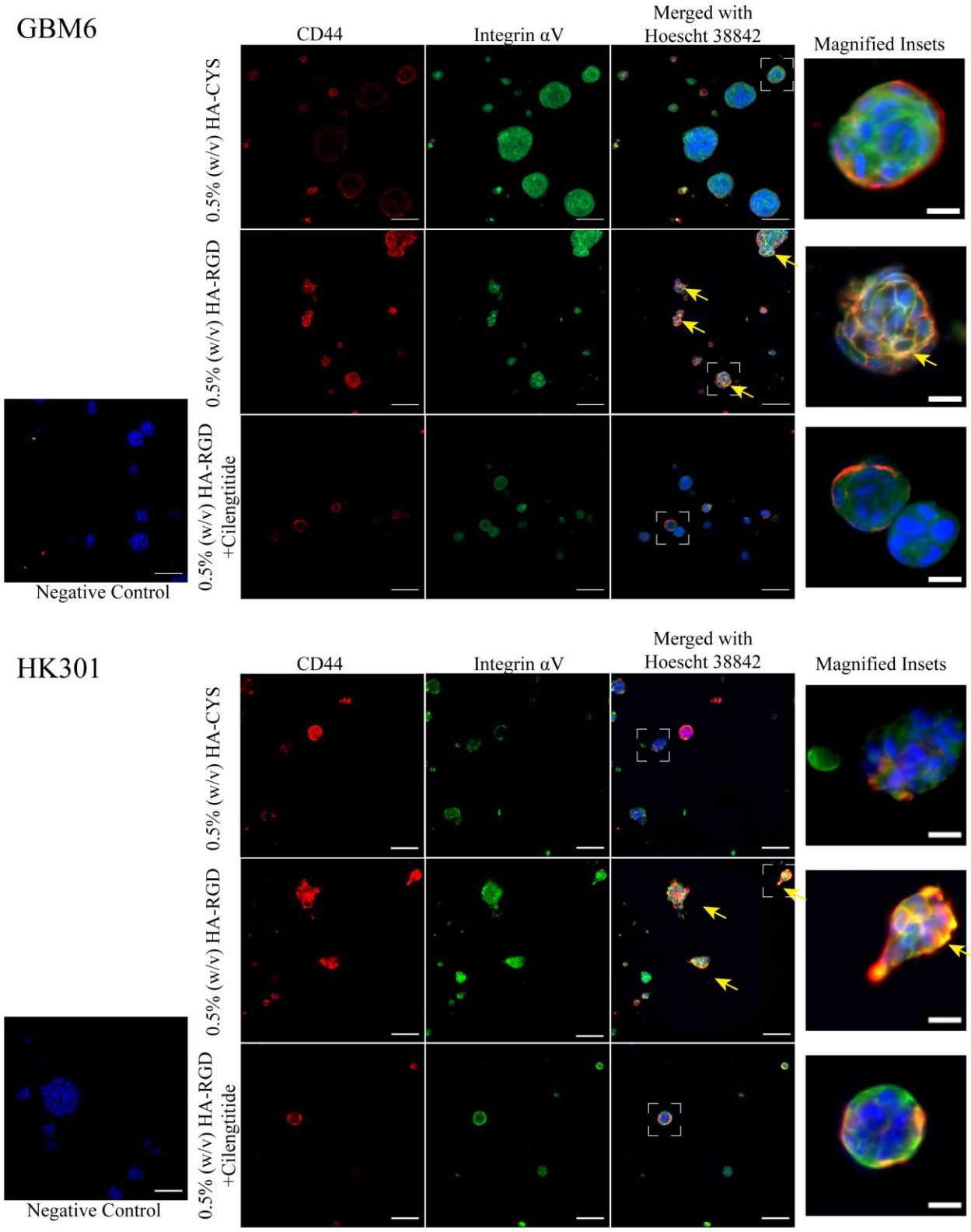

Figure 5

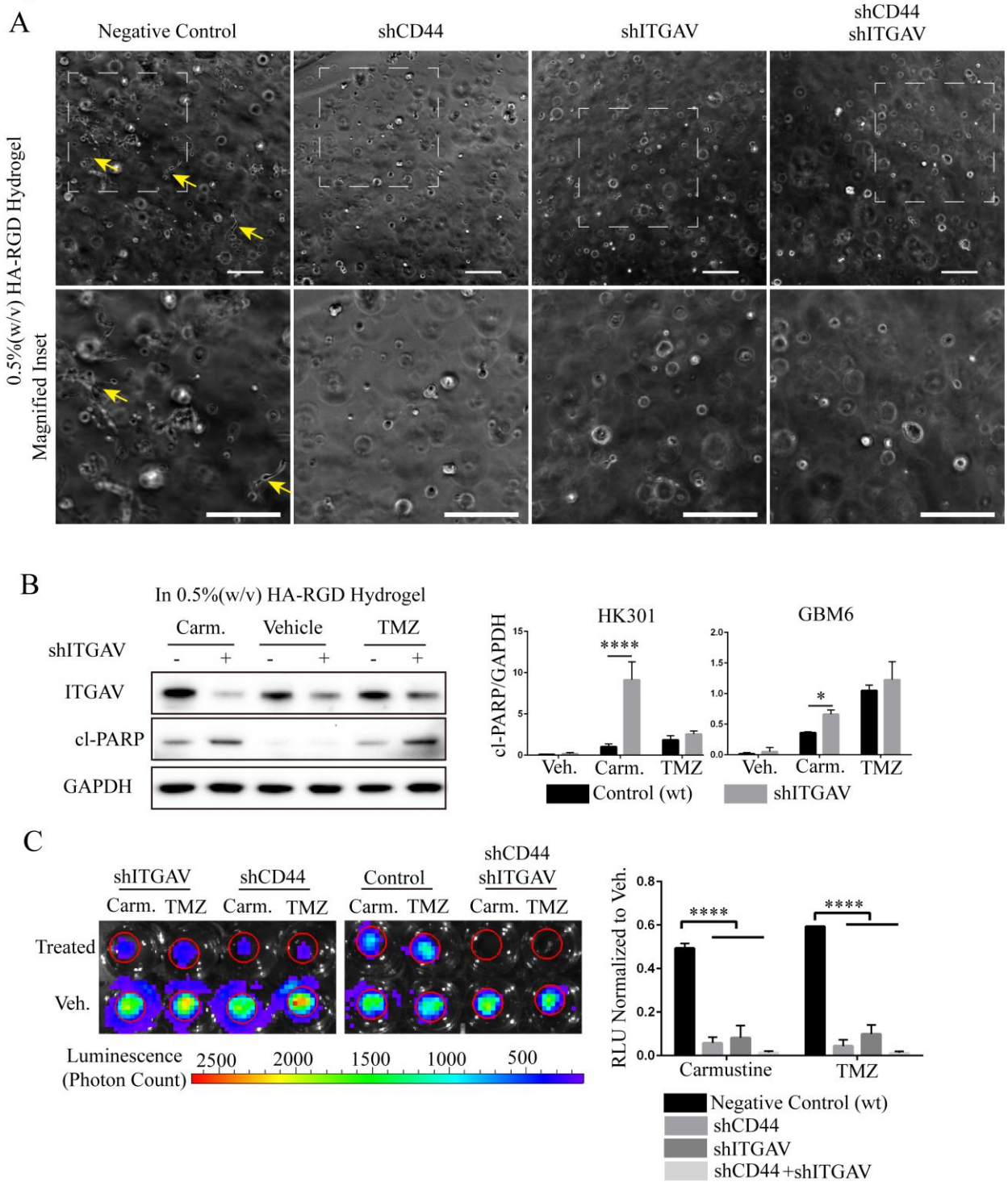

Figure 6

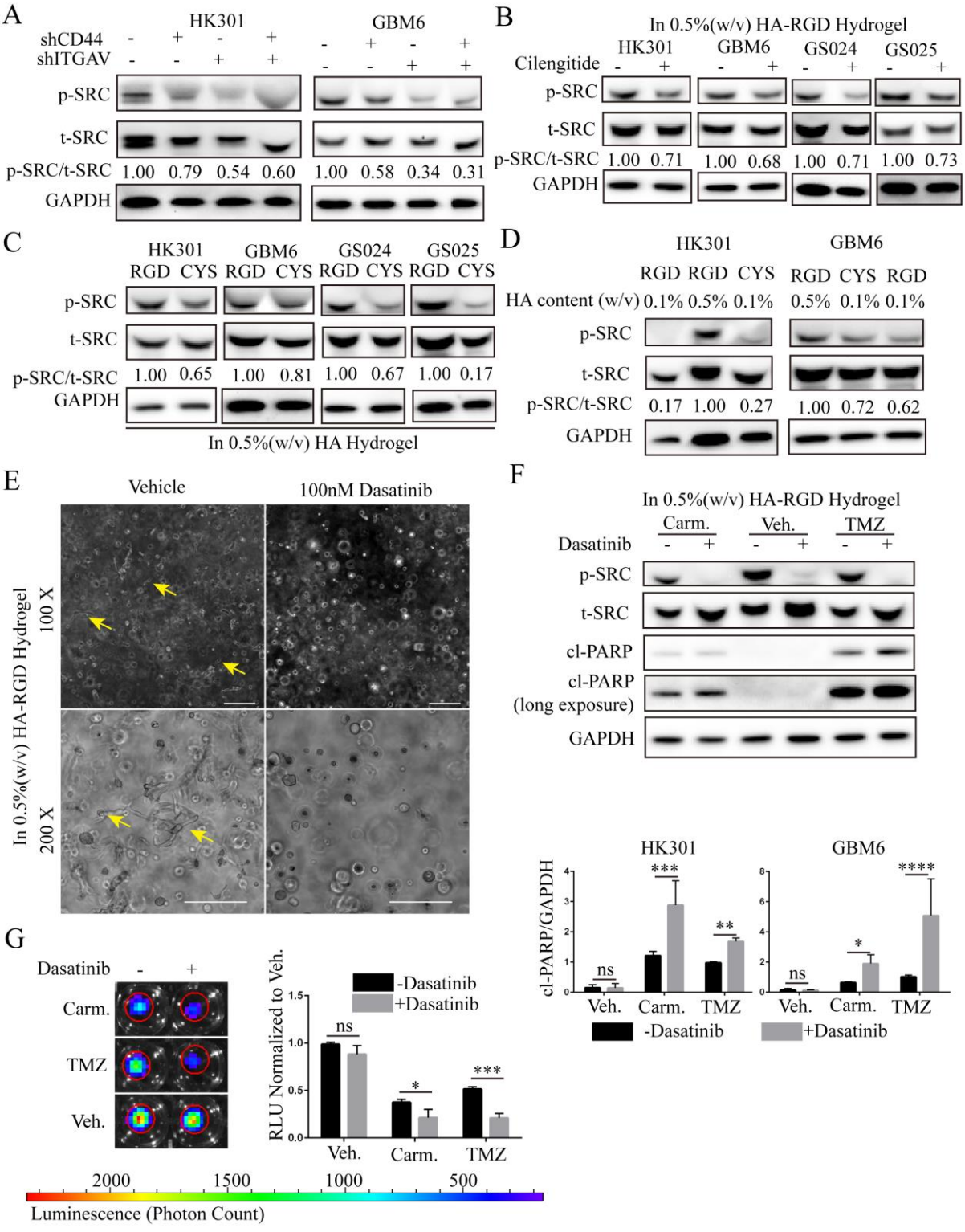

Figure 7

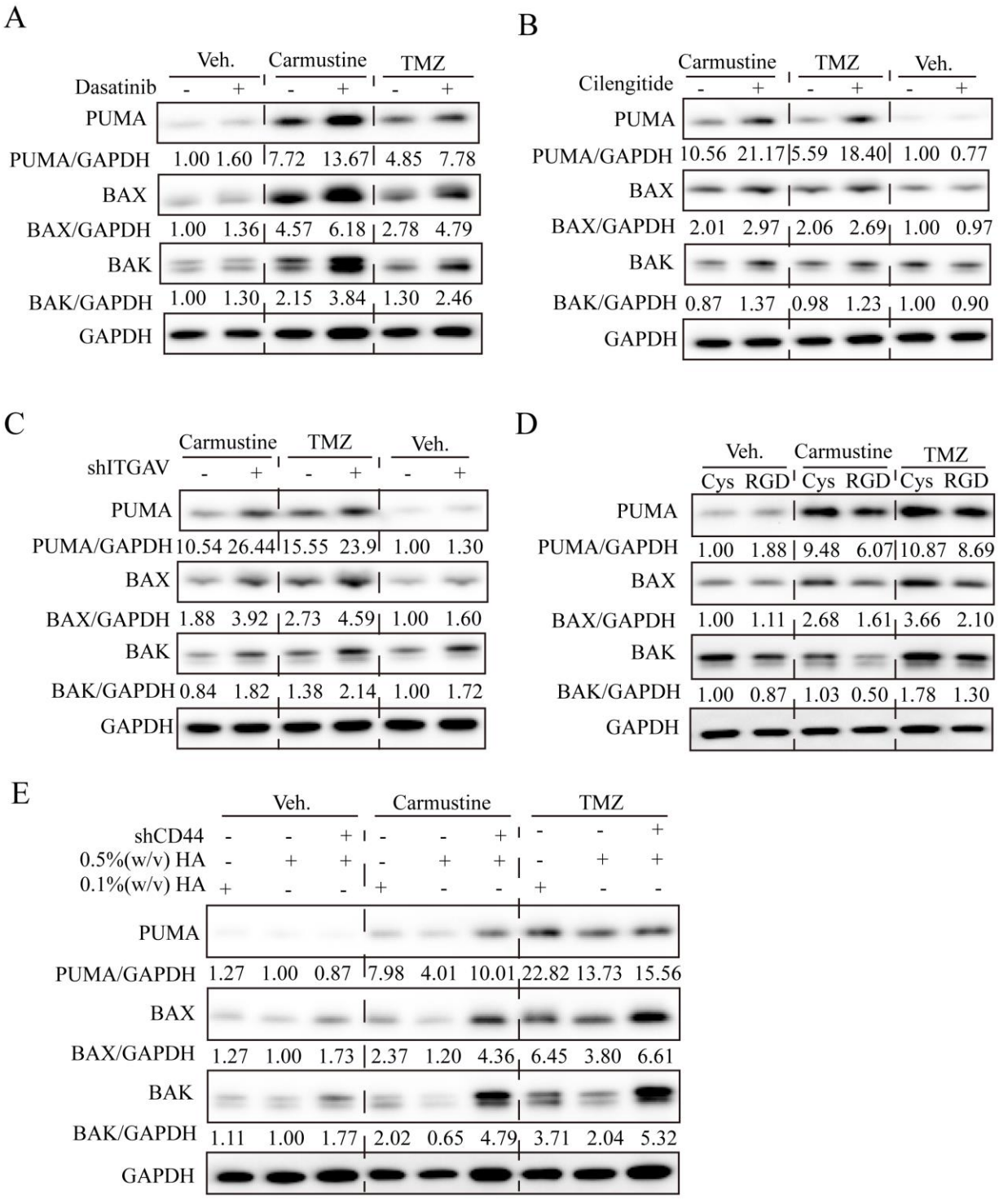

Highlights:

Hyaluronic acid (HA) and RGD-containing proteins in the extracellular matrix (ECM) interact with integrin and CD44 receptors, respectively, on patient-derived glioblastoma (GBM) cells to promote upregulation of Src in novel 3D hydrogel cultures.

Matrix-mediated Src activation promotes invasive morphologies and deregulates expression of pro-apoptotic factors induced by chemotherapies in GBM.

HA and adhesive proteins in the ECM protect GBM cells from chemotherapy-induced apoptosis.

Combinatorial treatment with chemotherapy dasatinib, which inhibits Src phosphorylation, provides a promising strategy to overcome matrix mediated drug resistance in GBM.